Some Basic Properties of Ice Dynamics

J.-C. Li*

Department of Physics, UMIST, PO Box 88, Manchester, M60 1QD, UK

M. Leslie

CCLRC, Daresbury Laboratory, Daresbury, Warrington WA4 4AD, UK

Received: October 11, 1996; In Final Form: April 17, 1997[⊗]

By use of inelastic incoherent neutron scattering techniques on ISIS at Rutherford-Appleton Laboratory, neutron spectra for a large range of recoverable high-pressure phases of ice have been measured. In order to understand the physical significance of the measured spectra and reproduce the experimental data, we have proposed a model, that requires two strengths of hydrogen bonding. In this paper, we describe some aspects of this model in detail and compare it with the existing potential models.

1. Inelastic Neutron Scattering Techniques

Thermal (or subthermal) neutrons are an excellent probe of studies of vibrational dynamics for a given solid and liquid, because several remarkable properties make thermal neutrons unique: for instance, the thermal neutron energy is comparable to phonon energies, and the wavelength associated with the neutron is of the same order as the interatomic distances in condensed phases. Another characteristic of this probe is that the neutron mass is of the same order as the mass of the scattering nuclei. The scattering is, therefore, sensitive to the structure and dynamics of the system. Hydrogen-bonded systems, such as water/ice, are a particularly suitable use of inelastic incoherent neutron scattering (IINS) because hydrogen has a large incoherent scattering cross section (at least an order of magnitude larger than other elements). Another advantage of using IINS techniques is that the intensity of the scattering is directly proportional to the vibrational amplitude weighted phonon density of states, which can be precisely calculated by using lattice and molecular dynamic techniques. Although ice has been measured using IINS in the past,[1−3] lack of intensity and resolution of scattering instruments made the data analysis and modeling very difficult. In recent years with increasing neutron flux at a number of sources and improving resolutions of inelastic scattering instruments, we can now measure the IINS spectrum with 1−2% ($\partial E/E$o) accuracy, which is comparable to IR and Raman techniques.

In order to obtain physical significance from the quantities measured using the neutron scattering technique, the spectrum has to be converted to one-phonon density of states (PDOS). This not only requires precise measurements of scattering background, empty container, etc., but also needs careful data treatment to remove multiphonon and multiple scattering contributions. The multiple scattering contributions can be eliminated by using a thin sample. The aim is to ensure that the scattering transmission from the sample is no less than 90% (i.e., no more than 10% of the total scattering from the sample).[4] The multiphonon scattering contribution could be significant for measurements carried out at high temperatures and large neutron momentum transfers. Therefore, it is important to make a good determination of the multiphonon scattering contributions and to remove them from the experimental data. One common method used for the calculations of the multiphonon scattering is the iterative technique.[5] The process of the calculation assumes that the IINS spectrum at the lower energy transfers is the one-phonon term and then calculates the multiphonon terms for the whole energy transfer region based on the one-phonon term. A new one-phonon spectrum is obtained by subtracting the calculated multiphonon contribution from the measured spectrum. This new one-phonon spectrum will then be used again for next iterative calculation of multiphonon terms, until convergence is reached after a few such iterations.

Figure 1 shows the measured IINS spectrum and the calculated one-phonon and multiphonon scattering contributions for ice Ih. Because the measurements were carried out at very low temperatures (∼15 K), the temperature effect is insignificant, and hence the multiphonon contribution is not great at the translational modes region (i.e. at low Q region) as shown in the figure. However, at the higher energy transfer of >100 meV the scattering is predominated by the multiphonon terms. This is due to large Q values in this region, resulting from the specific instrument design of TFXA at Rutherford-Appleton Laboratory (RAL).[6] (In order to measure the modes at high energy transfers, HET or MARI at RAL will be used.[7,8]) In return, we get very high resolution at low energy transfer which no other inelastic neutron scattering instruments can match.

The high-quality PDOS spectra obtained from TFXA[9] can be seen in a number of ways; first, the sharpness of the energy cutoffs of the two molecular optic modes and librational band clearly demonstrate the resolution of the instrument used; second, the initial curvature of acoustic band from 0 to 7 meV is in good agreement with the Debye behavior, i.e., $G(\omega) \sim \omega^2$. Hence, the detailed features of the acoustic band can be fitted precisely by a simple lattice dynamical (LD) model, indicating that the data were properly weighted from all q points of the first BZ in the reciprocal space. These measurements unambiguously provide an ideal condition for theoretical simulations. In this paper, we present detailed studies of a number of effects of pair potentials and theoretical models on the resulting PDOS, such as the long-range interaction effects of a pair potential, effects of the polarized properties of potentials, and effects of the proton disordering which are all vitally important for us to understand the dynamical properties of ice.

[⊗] Abstract published in *Advance ACS Abstracts,* July 15, 1997.

S1089-5647(96)03246-4 CCC: $14.00

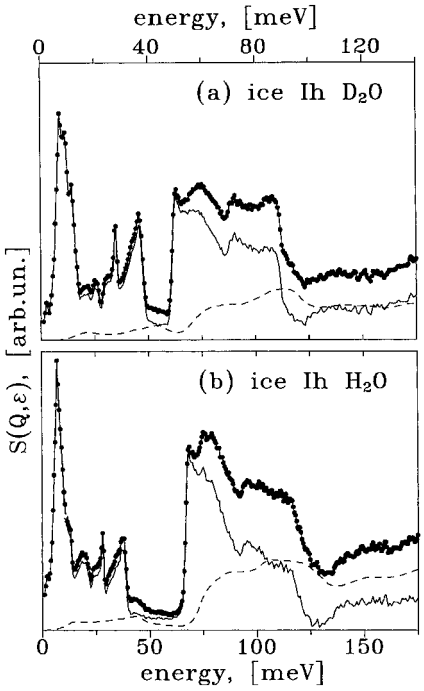

Figure 1. The solid line though the data points is the measured spectrum for ice Ih; the continuous line is the one-phonon term calculated, and the dashed line is the multiphonon contributions.

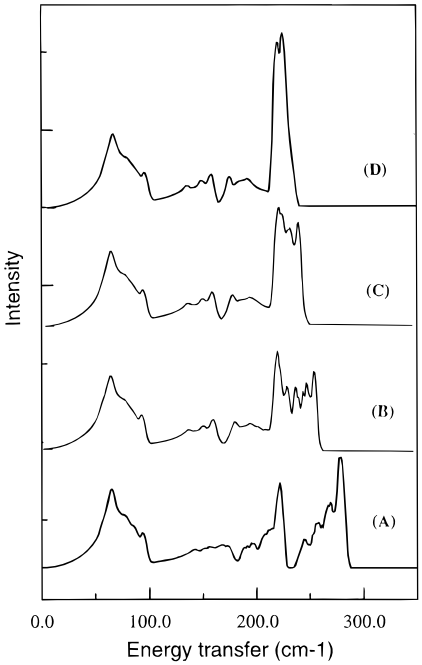

Figure 2. Comparison of calculated PDOS for a supercell of 16 water molecules with different ratio of the hydrogen-bond force constants K_1:K_2 (the weak bond force constant K_2 is fixed, having a value of 1.1 eV/Å^2): the curve (A) is for the ratio of 1.8, (B) for 1.5, (C) for 1.3, and (D) for 1.0. The O−O−O bending force constant, 0.56 eV/θ^2, is fixed for all calculations.

2. Effects of Long-Range Interactions and of the Polarized Potential

The long-range interactions, mainly from Coulomb charge interactions, have been considered the main effect on the feature observed in the 25−40 meV (200−320 cm^{-1}) region based on the measured dielectric constant; this effect would result in the TO/LO splitting in the translational modes region, and it has therefore been extensively discussed by Klug and Whalley.[10] However, there have been no other independent measurements to confirm the effects. Many IINS spectra for different forms of ice, such as ice in pores and ice as small droplets, indicate that the long-range interactions cannot be responsible for the unusual features seen in their PDOS (i.e., the two triangular shapes of optic modes). In order to study the long-range effects, we calculated the PDOS using a number of different water−water potentials which are often used in the structure determination and other areas, such as the TIP4P,[11] MCY,[12] and KKY[13] potentials. The reason we chose these potentials is that, on one hand, the TIP4P is a potential having a very simple Lennard-Jones core combined with a typical three point charge term which is shared by many other potentials; for MCY, it is also a three point charge potentials with exponential forms of hard core. On the other hand, the KKY potential is a complicated nonrigid water molecular potential that gives a full range of vibrational frequencies, including intermolecular and intramolecular modes up to 420 meV. Comparison between molecular dynamic (MD) calculations using these potentials,[14] which have a range of interactions up to 10 Å, and LD calculations based on a set of force constants among the nearest-neighboring waters obtained from these potentials shows that the long-range interaction effect to the PDOS is insignificant in the translational region.[15]

3. Effects of the Ratio of the "Strong" and "Weak" Force Constants

As we indicated above, in order to reproduce the two triangular shapes of strengthening molecular optic modes for ice Ih/Ic, we have to use two strengths of H-bond force constants. Although the existing potentials provide some degree of orientational differences in energy and force constants (see table 1 in ref 15), they are not large enough to separate the vibrational frequencies that are associated with the strong and weak bonds (i.e., decouple from each other). We found that they tend to produce a single peak in the intermolecular optic region. In order to demonstrate this point, we have made a series of calculations for the PDOS with different ratio of K_1:K_2. (Other force constants are kept the same as listed in Table 2 of ref 15). Figure 2 shows the series of calculations for a supercell of 16 water molecules with four different ratios of the force constants (the weak bond force constant K_2 is fixed for a value of 1.1 eV/Å^2), 1.8, 1.5, 1.3, and 1 (i.e., the strong and weak are the same value). The results show that, for the PDOS with the ratio less than 1.5, the two strengthening optic bands are starting to merge together. This means that the splitting phenomena can only be seen when the ratio of the strong/weak force constants among the nearest-neighboring molecules is greater than 1.5. As we indicated in an earlier section, the pair potentials we have tested so far show that the ratios are all less than this values. Indeed, if we assume that the orientational differences of the force constants come only from the charge terms based on the classic dipole−dipole interactions (including polarized potentials), it would be almost impossible to get the ratio greater than 1.5.

4. Effects of Proton Disordering

In order to represent the proton-disordered structure for ice Ih, large supercells are needed. As we know, for the primary cell with four molecules (*P*63/*mmc* for oxygen network), there are only two ways to arrange the protons without broking the Bernal−Fowler ice rules, i.e., two possible structural symmetries, namely, *Cmc*2 and *Cc*. In the *Cmc*2 structure, all the hydrogen bonds in the *C* axis are "strong" and all the bonds in basal plane are "weak" according to our early assignments.[15] For eight molecular orthorhombic cells, however, there are 17 arrangements of the protons; the strong and weak bonds can,

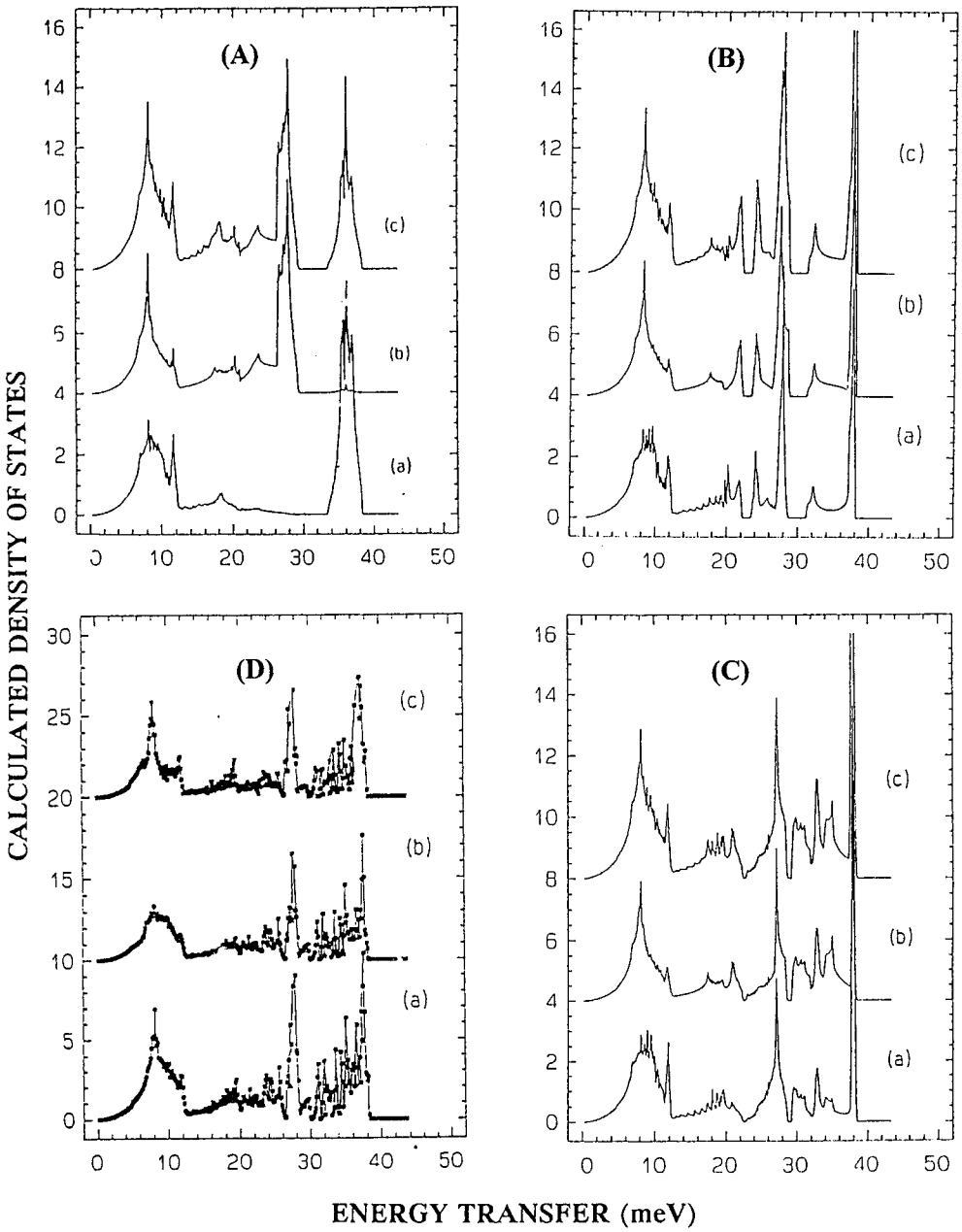

Figure 3. Plot showing a series of calculations of PDOS using the different sizes of the ice Ih lattice to represents the proton disordering: (A) for a lattice cell with 4 molecules (*Cmc*2 structure), (B) 8 molecular structure, (C) 16 molecules, and (D) 32 molecules. Curve a is the integrated phonon density involving the vibrations in the *c* axes, curve b is for the phonon density integrated normal to *c* axes, and curve c is the total phonon density of states, which is the sum of (a) and (b).

therefore, be mixed in an ordered way.[16] Figure 3 shows a series of LD calculations for a number of structures based on the two force constant model.[15] The first set of curves (A) are the PDOS for the *Cmc*2. Because, in this structure, all bonds in *c* axis are the strong bond and all bonds in the basal plane are the weak bonds, we therefore see that the peak at 28 meV appears only in the integrated modes associated the vibrations in basal plane and the peak at 37 meV appears only in the *c* axis of hexagonal structure. The total PDOS has both peaks as seen in the calculated spectrum by Carido et al.[17] Although the peak positions are correct, the shape of the calculated spectrum does not agree with experimental data—the two peaks are very sharp and well separated from one another.

When a large unit cell with eight molecules was used (other properties, such as force constants, are the same), we can see the improvement in the calculated results as shown in curves (B). Because the strong and weak bonds are present in both crystal orientations of the sample (i.e., *c* axis and basal plane), we therefore see the two peaks in both spectra. Another important improvement is that more phonon frequencies are shown in the gap between the peaks which will gradually build up the shape as seen in the measured spectra. When the lattice cell increases to 16 molecules, the resulting spectra begin to look very much like the measured spectrum as shown in curves (C). The final set of calculations is for a supercell of 32 molecules. In this cell, the protons can be reasonably well mixed in all directions. The two optic peaks merge into one.

From these series of calculations, we could demonstrate that the unusually triangular shapes of the two optic peaks can be represented by the proton disordering and the integrated intensities of the two peak areas are directly proportional to the ratio of the numbers of the strong and weak bonds in the structure. If we assume the protons are completely disordered, the ratio of strong (from the bonds with oblique symmetries) and the weak (from the bonds with mirror symmetries) bonds conforms well with the ratio of the intensities (i.e., 2:1).

Ice Ih is a completely proton disordered system. In order to truly represent a proton disordered structure, an infinite lattice is needed. In reality, it is not possible for us to carry out such calculations. In fact, if the superlattice is large enough to satisfy a number of conditions—(1) the averaged total dipole momentum is near zero from sampled possible proton arrangements, (2) the calculated structural factors are converged, and (3) the calculated PDOS are converged, i.e., further increase of the lattice cell would cause no changes in the calculated results—we can then believe that the structure used is a good representation of the proton disordered structure, such as ice Ih.

In order to produce proton-disordered ice structures for the LD calculations, analysis of all possible combinations of the proton arrangements in different sizes of supercells is necessary. If we assume that the protons in ice Ih/Ic structures are entirely disordered, the strong- and weak-bond configurations will have a ratio of $^2/_3$:$^1/_3$ based on the assumption in ref 14. However, if the unit cell is small (with periodic boundaries), the ratio is quite different for topological reasons. For instance, for the primary cell, the structure of ice Ic contains weak bonds only. The ratio of strong/weak bonds gradually increases to the statistical value of $^2/_3$:$^1/_3$ when the size of the lattice increases. On the other hand, if protons in the ice structures are completely disordered, one would expect that about 20% of water molecules have either four strong or four weak bonds surrounding them. (Other possible combinations for each molecule are 1 strong and 3 weaks, 2 strongs and 2 weaks, and 3 strongs and 1 weak.) These entirely strong- or weak-bonded clusters (one water molecule at center) would have quite different dynamical properties due to strong coupling with the neighboring molecules. In order to clarify this point, lattice dynamical calculations have been made for a number of different proton disordered structures with 32 and 64 water molecules. Some structures have a fraction of molecules with four identical bonds (i.e., 4 strong or 4 weak bonds), and others will have no or a very small number of such clusters. The calculations show that the structures which contain the clusters with identical bonds will not reproduce the triangular shapes of optic peaks in IINS spectra well, while the structures having no (or very few) such clusters do. This is because the triangular shape of optic modes is due to decoupled optic modes (i.e., modes have very little dispersion). This is owing to the fact that the strong/weak bonds have broken the continuity of the system; the molecular optic modes or the dispersion curves are rather flat. This studies could have considerable implications in a number of areas, because, by removing the four identical bond clusters from the structure, one could allow the electrons to redistribute from one bond to another (weak to strong, for instance, or rehybridized), which causes the split of the H-bond strengths. Also, the removal of the clusters would result in the increase of the connectivity of the strong- or weak-bond networks (instead of lumping together). These networks are very similar to the percolation networks proposed by Stanley and Teixeira.[18] This observation may be relevant to the understanding of a number of particular properties of ice, such as the high sound velocity.[19]

5. Summary

From the above calculations, we could conclude that the two hydrogen-bonding force constants are the basic requirement for reproducing the measured spectrum. If a water−water potential contains these large different force constants, it will produce the same effect as seen from the two force constant model. Since the anisotropic properties of the classic potentials are a result of the charge interactions, one could exaggerate its effects by using a larger O−Om distance or a larger effective charge. This approach could result in four different H-bond force constants, instead of two required for the calculation. If the strong hydrogen bonding is from the configurations of oblique symmetries (the weak bonds are from the mirror symmetries), it would be further apart from the concept of charge effects, because the obliques are the two middle strengths among the four configurations from the dipole−dipole interaction point of view (see Table 1 in ref 15), and it can, therefore, only be attributed to the quantum mechanical effect.

Acknowledgment. The authors thank the Engineering and Physical Science Research Council (UK) for financial support and the Rutherford-Appleton Laboratory for the use of neutron facilities.

References and Notes

(1) Prask, H. J.; Trevino, S. F.; Gault, J. D.; Logan, K. W. *J. Chem. Phys*. **1972**, *56*, 3217 (1972).

(2) Renker, B. In *Physics and Chemistry of Ice;* Whalley, E.; Hones, S. J.; Gold, L. W., University of Toronto Press: Toronto, 1973; p 82.

(3) Klug, D. D.; Whalley, E.; Svenson, J. H.; Root, J. H.; Sears, V. F. *Phys. Rev. B.* **1991**, *44*, 841.

(4) Skold, K.; Price, P. L. Eds. *Neutron Scattering in Methods of Experimental Physics*; Academic Press: New York, 1986; Vol. 23.

(5) Kolenikov, A. I.; Sheka, E. F. *Sov. Phys. Solid States* **1983**, *25*, 1303.

(6) Boland, B. C. ISIS Experimental Facilities, Rutherford Appleton Laboratory, UK, 1990.

(7) Li, J-C.; Londono, J. D.; Ross, D. K.; Finney, J. L.; Bennington, S. M.; Tayor, A. D. *J. Phys.: Conddens. Matter* **1992**, *4*, 2109.

(8) Li, J-C.; Ross, D. K. *J. Phys.: Condens Matter* **1994**, *6*, 10823.

(9) Li, J-C.; Londono, J. D.; Ross, D. K.; Finney, J. L.; Tomkinson, J.; Sherman, W. F. *J. Chem. Phys.* **1991**, *94*, 6770.

(10) Klug, D. D.; Whalley, E. *J. Glaciol.* **1978**, *21* 55. Comment: *J. Chem. Phys.* **1979**, *71*, 1513.

(11) Jorensen, W. L.; Chandrasekhar, J.; Maura, J. D.; Impey, R. W.; Klein, M. L.; *J. Chem. Phys.* **1983**, *79*, 926.

(12) Matsuoka, O.; Clementi, E.; Yoshimine, M. *J. Chem. Phys.* **1976**, *57*, 1351.

(13) Kumagai, N.; Kawamura, K. K.; Yokokawa, T. *Mol. Simul.* **1994**, *12*, 177.

(14) Burnham, C. J.; Li, J-C.; Leslie, M. *J. Chem. Phys.*, in press.

(15) Li, J-C. Submitted to *J. Phys. Chem.*

(16) Howe, R.; Whitworth, R. W. *J. Phys. Chem. Solids* **1989**, *50*, 963.

(17) Criado, F. J. Bermejo, M. Carcia-Hernandez J. L Martinez, *Phys. Rev. E* **1992**, *47*, 3516.

(18) Stanley, H. E.; Teixeira, J. *J. Chem. Phys.* **1980**, *73*, 3404.

(19) Sette, F.; Ruocco, G.; Krisch, M.; Bergrmann, U.; Masciovecchio, C.; Mazzacurati, V.; Signorelli, G.; Verbeni, R. *Phys. Rev. Lett.* **1995**, *75*, 850.